

THE LOAD-DISPLACEMENT BEHAVIOUR OF GROUND ANCHORS IN FINE GRAINED SOILS

JURAJ CHALMOVSKÝ*, LUMÍR MIČA

Brno University of Technology, Faculty of Civil Engineering, Institute of Geotechnics, Veveří 331/95, 602 00 Brno, Czech Republic

* corresponding author: chalmovsky.j@fce.vutbr.cz

ABSTRACT. Ground anchors represent an important structural element in the area of geotechnical engineering. Despite their extensive usage, a design process of these elements is usually performed using simple empirical and semi-empirical methods, neglecting several important influencing factors. This paper gives an analysis of the factor of non-uniform distribution of skin friction resulting in a progressive failure of ground anchors. First, the finite element method in combination with a material model involving regularized strain softening is utilized. Next, an experimental program, including several investigation anchor load tests, was carried out. The goal of this program was to confirm preliminary conclusions drawn from numerical studies and to obtain relevant data for further back analysis. After, there is then described a newly developed application based on the load transfer method, in which all the findings from numerical computations and experimental measurements are incorporated.

KEYWORDS: Ground anchor, strain softening, investigation load test, load transfer function.

1. INTRODUCTION

Mobilization of shear stresses along a fixed length of ground anchors is significantly non-uniform during anchor loading. In the first loading stages, shear stresses mobilized at the grout soil interface are concentrated at the top of the fixed anchor length. After reaching the peak value, shear stress is consequently reduced towards its critical and residual value. The location of peak shear stress moves along the fixed anchor length as schematically shown in Figure 1. The non-constant (peak) shear stress distribution along the fixed anchor length has been experimentally confirmed by several authors: Ostermayer [1], Scheele [2], Barley [3], Woods, and Barkhordari [4]. The described phenomenon has a severe influence on the ultimate bearing capacity, ground anchor efficiency and load displacement curves. The ultimate load carrying capacity is not directly proportional to the fixed anchor length. Because the maximum bond stress is reached only in a small portion of the fixed anchor length, anchors with fixed lengths longer than 8 m are inefficient (Barley [5]). In addition, the assumption of a constant bond stress may lead to an overestimation of the load carrying capacity.

Based on regression analysis of anchor loading tests performed mainly in London clay and glacial clay, Barley [3] has proposed an analytical formula for the efficiency factor f_{eff} and for the load carrying capacity of low pressure grouted anchors T_{ult} (Eq. 2), where L_{fixed} is the fixed anchor length, D is the borehole diameter and c_u is the undrained soil shear strength. The progressive failure mechanism is dominant in the case of stiff, to very stiff over-consolidated clays and dense, to very dense non-cohesive soil exhibiting peak

shear strength followed by a strength reduction during strain softening towards a residual stress state.

$$f_{eff} = 1,6L_{fixed}^{-0,57} \quad (1)$$

$$T_{ult} = \pi DLf_{eff}c_u \quad (2)$$

2. FINITE ELEMENT MODELLING

In order to analyze the effect of progressive failure by numerical methods it is necessary to adopt a constitutive model involving post-peak strain softening. For this purpose the Multi-laminate Model for Stiff Over-consolidated Clays (MLSM) proposed in Schadlich [7] was used. MLSM requires 11 input parameters: the oedometric reference stiffness $E_{oed,ref}$, the modulus of elasticity for unloading reloading $E_{ur,ref}$, the Poisson ratio for unloading reloading ν_{ur} , the shear hardening parameter A_{mat} , the critical state friction angle φ_{cs} , the Hvorslev surface inclination φ_e , the initial pre-consolidation pressure σ_{nc} , the reference pressure p_{ref} , the stress dependency index m , the softening scaling factor h_{soft} , and the internal length l_{calc} . Ground conditions of modeled and tested anchors consist of highly over-consolidated stiff Brno clay of the Neogene age. Svoboda, Mašín [8] estimated the value over-consolidation ratio $OCR=6.5$ based on oedometric tests on non-disturbed samples. Applying the formula proposed by Mayne, Kulhawy [9] leads to $K_0=1.25$. Input parameters for MLSM are calibrated based on three CU triaxial tests (Svoboda et al. [10]) performed at different confining pressures (275 kPa, 500 kPa, 750 kPa). The calibration process is divided

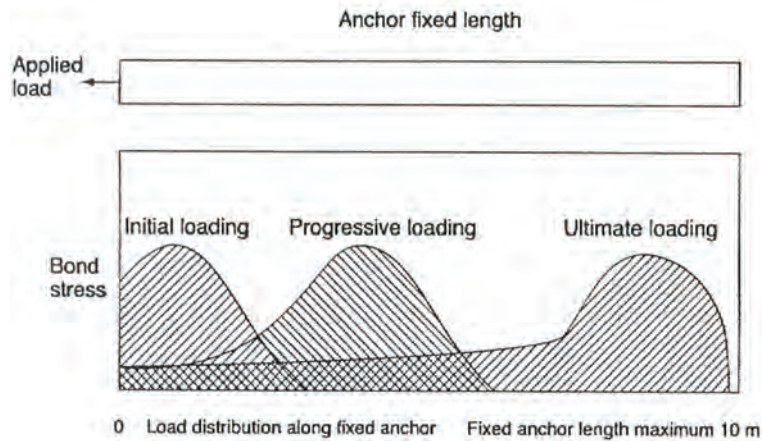


FIGURE 1. Non-uniform shear stress distribution along the anchor fixed length [6].

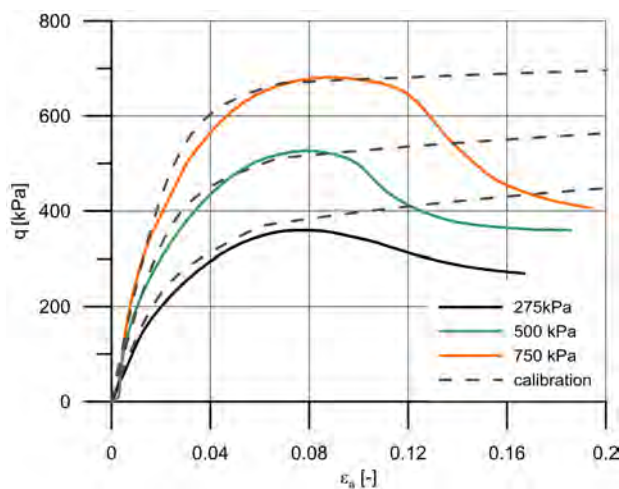


FIGURE 2. Triaxial stress strain curves.

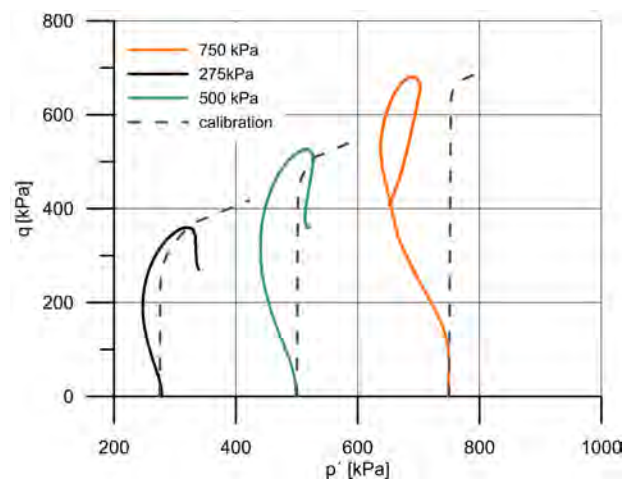


FIGURE 3. Effective stress paths.

into two parts described in the following sections. MLSM with determined input parameters is then applied to simulation of a low pressure (gravity) grouted anchor. Finally, back analysis of the investigation anchor load test is performed. FEM packages Plaxis 2D Brinkgreve et al. [11] and Plaxis 3D Brinkgreve et al. [12] were used for the analyses presented here.

2.1. STRAIN HARDENING PARAMETERS

First, parameters governing strain hardening plasticity were obtained (Table 1). This can be done using a "single stress point approach". SoilTestLab application was used for this purpose. Comparisons between simulations on a single stress point level and measured data (stress strain curves and effective stress paths) are shown in Figure 2 and Figure 3.

2.2. STRAIN SOFTENING PARAMETERS

Determination of parameters governing strain softening on a single stress point level is not possible, as the softening rate is size dependent and non-homogeneity (shear band) originates in a sample. A 3D model of a triaxial test with real sample dimensions is therefore

necessary. The strain softening behaviour is governed by two parameters: the softening scaling factor h_{soft} which controls the rate of softening for a given damage strain increment and the internal length l_{calc} which determines the domain to be considered during the regularization. In order to transfer a calibrated softening rate into a boundary value analysis, softening scaling (Brinkgreve [13], Galavi [14]) can be utilized because the softening rate depends only on the ratio h_{soft}/l_{calc} . For the purpose of calibration of these parameters, a 2D plane strain numerical model of a biaxial test and a full 3D numerical model of a triaxial test were employed.

Measured and predicted stress strain curves for the CU test with confining pressure 275 kPa (closest to the stress range in the anchor vicinity) are shown in Figure 4. Three simulations of a biaxial test with different h_{soft}/l_{calc} ratios (8000, 24000, 32000) were performed. A ratio of $h_{soft}/l_{calc}=32000$ is used in the final prediction with a 3D triaxial test model and for further finite element models. Localization of shear strains into the shear band at the end of the simulation is clearly visible in Figure 5. In the case of

$E_{oed,ref}$ kPa	$E_{ur,ref}$ kPa	ν_{ur} -	A_{mat} -	ϕ_{cs} °	ϕ_e °	σ_{nc} kPa	p_{ref} kPa	m -
1200	8000	0.2	15	20	16	1800	100	0.55

TABLE 1. Values of input parameters governing strain hardening.

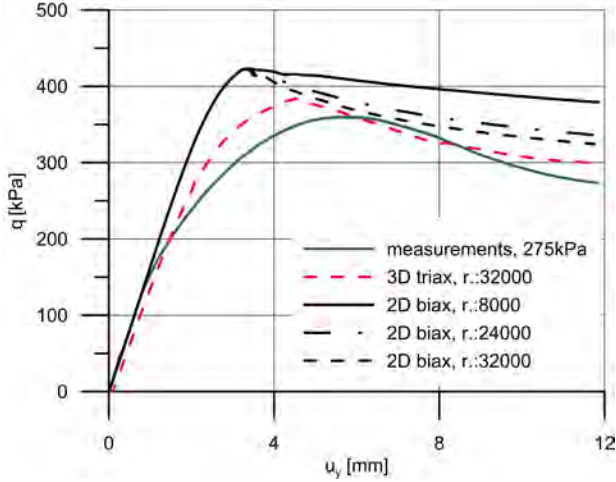


FIGURE 4. Triaxial stress strain curves – softening.

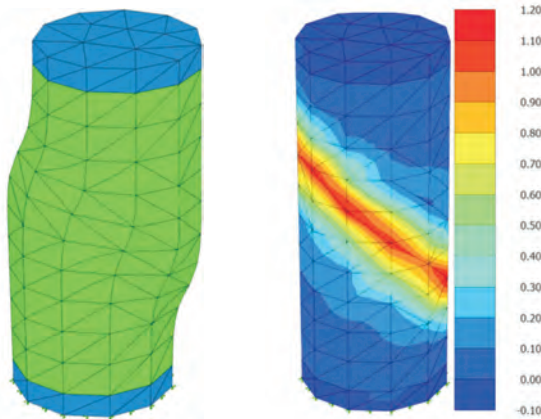


FIGURE 5. Post peak behaviour.

solving a practical boundary value problem, the internal length l_{calc} is appropriately selected (according to the recommendations) and h_{soft} is scaled to get the required h_{soft}/l_{calc} ratio.

2.3. INITIAL APPLICATION

In the first step after calibration, an FE – MLSM combination was used for simulating a load test of the gravity grouted anchor with a fixed length L_{fixed} of 4 m. The axisymmetric finite element model using 6-noded triangular elements was prepared. Mobilization of skin friction along the fixed length on the grout-soil interface for three different load levels (65 kN, 125 kN, 146 kN) is shown in Figure 6. After reaching the peak skin friction of 95 kPa in the second load step, shear stresses are decreasing towards the critical

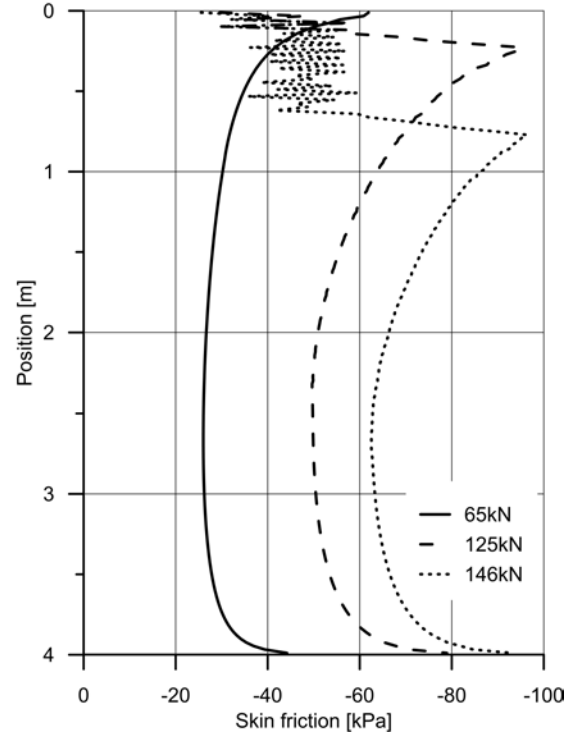


FIGURE 6. Shear stress distributions for different loading stages.

value. With increasing load level, also the fixed length section in the softening regime is growing.

2.4. BACK ANALYSIS OF THE INVESTIGATION ANCHOR LOAD TEST

Calculations adopting a simple model of a ground anchor confirmed that it is possible to model the progressive failure mechanism by combination of the finite element method and the constitutive model involving regularized strain softening. In the second step, back analysis of the investigation anchor load test was therefore performed. The investigation load test was carried out by Misove [15]. The free and fixed length was 4 m and 8 m, respectively. The anchor was post-grouted by Tube-A-Manchette system (TAM). Both section were separated by a packer to prevent a grout inflow into the free length. The anchor was excavated after the test in order to determine its diameter. Due to post-grouting, the diameter was enlarged from the original 140 mm to 190 mm. The process of grouting was modelled by applying a pre-calculated volumetric strain to the respective elements thus increasing radial stresses acting on the fixed length surface. Three basic calculations were performed:

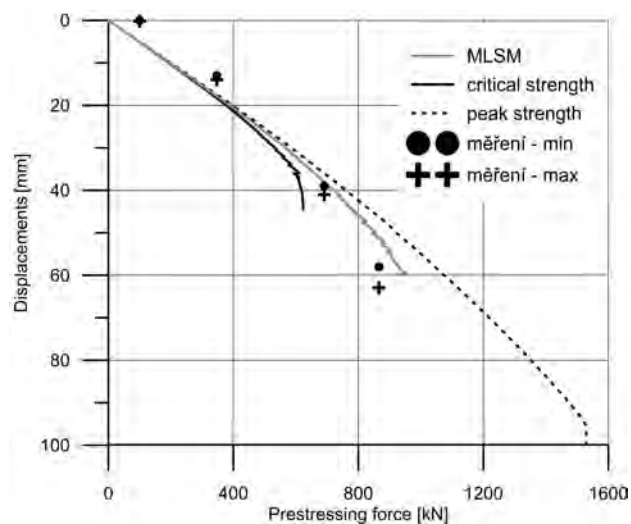


FIGURE 7. Predicted and measured load – displacement curves.

- Standard calculation with MLSM involving the reaching of peak shear strength (Hvorslev surface) followed by strain softening.
- Calculation with modified version of the MLSM with no peak strength, thus only critical shear strength can be reached.
- Calculation with the standard Mohr – Coulomb model with peak shear strength parameters $c_p=90$ kPa and $\varphi_p=14^\circ$. These values were determined from the shear box test assuming a normal stress acting on a fixed length surface between 200 and 400 kPa.

Predicted and measured load – displacement curves are shown in Figure 7. The alternative using peak strength characteristics significantly overestimates the bearing capacity. On the other hand calculation with modified MLSM (only critical strength can be reached) underestimates the bearing capacity. A sufficient match in terms of displacements and the carrying capacity is only reached when a skin friction decrease from peak to critical is involved. Predicted shear stress distributions for three different load levels (627 kN, 739 kN, and 800 kN) are shown in Figure 8. Skin friction mobilization is significantly non-uniform. Progressive shear stresses decrease from the peak value of 150 kPa and gradually propagate to a distance of 3 m from the fixed length head.

3. EXPERIMENTAL PROGRAM

Analysis performed using the combination of FEM and MLSM has revealed that neglecting a progressive skin friction decrease may lead to highly inaccurate results. It was therefore decided to perform a detailed experimental test program involving 6 investigation load tests (up to a failure) of anchors constructed in Brno neogene clay. Each anchor was monitored by two groups of systems:

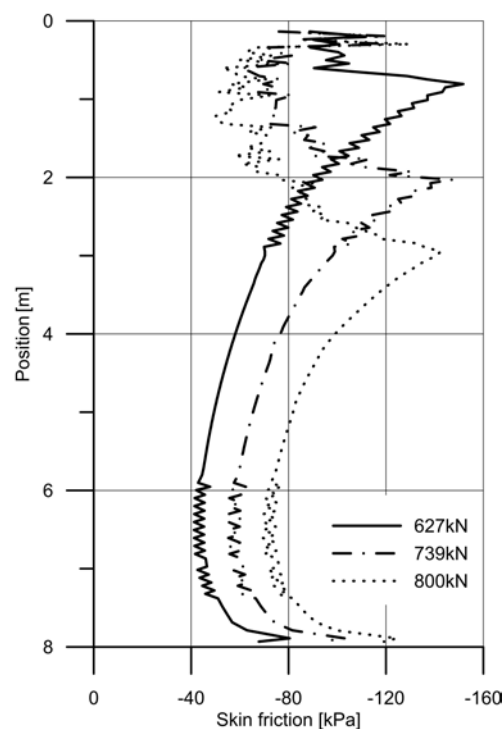


FIGURE 8. Computed shear stress distributions for three load levels.

- Standard monitoring: measuring of anchor head displacement (LVDT) and a pre-stressing force.
- Detailed monitoring: axial strain measuring along the tendon and in grout, using vibrating wire tensometers and electric resistance gauges.

In sum 5 of the tested anchors were standard temporary anchors, the last one was SBMA (Single Bore Multiple Anchor). The free length of standard anchors was 5 m, the fixed length was 6 m (2 tests), 8 m (1 test) and 10 m (2 tests). Due to the limited extent of the paper only two representative results are presented. Detailed test results and their interpretation can be found in Chalmovský [16]. The time record of a measured pre-stressing force and the anchor head displacement is shown in Figure 9. On reaching the ultimate bearing capacity (point no. 1) there followed a rapid decrease of pre-stressing force which was accompanied by clearly visible upward movement of the grout body. The anchor was fully unloaded after that (point no. 2) followed by re-increasing of prestressing force. It was found that the bearing capacity dropped to 55% of the original peak value (point no. 3). At this load level anchor head displacements stabilized (point no. 4). Similar behaviour was observed on all tested anchors. Taking into account that the tendon – grout interface was not broken, it might be concluded that the observed behaviour was a consequence of rapid progressive failure of the grout-soil interface.

The second example (Figure 10) presented in this paper are measured distributions of pre-stressing force along the fixed length of the anchor ($L_{fixed}=10$ m). It is obvious from this figure that for three initial

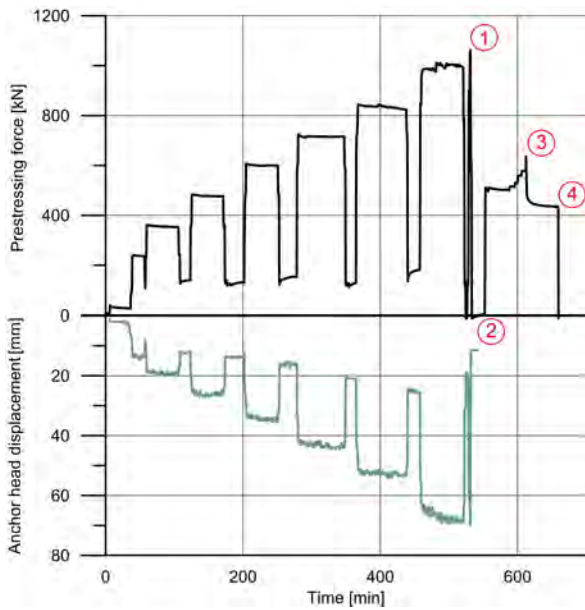


FIGURE 9. The investigation test record.

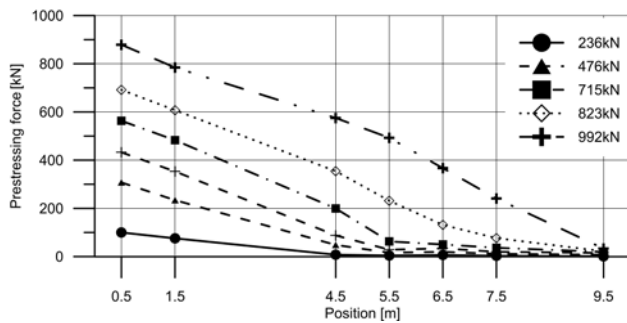


FIGURE 10. Measured distributions of pre-stressing force.

load levels (236 kN, 476 kN, 715 kN) only the first 5.5 m of the fixed length is utilized. Considering that pre-stressing force of 715 kN is much higher than what would be considered as a design bearing capacity (applying standard design methods), the anchor economic efficiency is low.

4. DEVELOPMENT OF APPLICATION BASED ON LOAD-TRANSFER FUNCTIONS

Analysis using the finite element method and experimental results confirmed that the progressive decrease of skin friction along anchor fixed lengths significantly influences an overall load – displacement behaviour and an ultimate bearing capacity of anchors. Despite its complexity, numerical analysis with a constitutive model involving regularized strain softening, presents a time demanding task. In order to involve the aspect of a non-uniform shear stress distribution and other factors in a design process, an approach incorporating the load transfer method is therefore proposed. A load transfer function (t - z curve) is the dependence of shear stress mobilized on the surface of a fixed length seg-

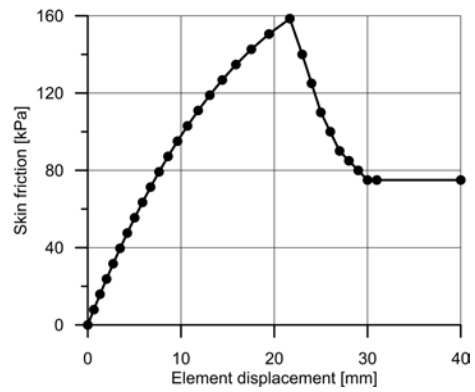


FIGURE 11. Assembled load transfer function.

ment and its vertical displacement. The load transfer method is frequently adopted for the determination of load settlement curves of vertically loaded piles (Coyle, Reese [17], Coyle and Sulaiman [18]). However its use for ground anchors is rare. The important feature (from a practical point of view) of the proposed approach is that the load transfer function shape is determined using standard laboratory tests. No prior loading tests are necessary. The newly developed algorithm includes the following main features:

- Derivation of load transfer functions from laboratory testing following the procedure stated in Kraft et al. [19].
- Axial stiffness change due to the occurrence of tensile cracks in the grout material ([20]).
- Radial stress increases due to the post-grouting. Therefore, cylindrical cavity expansion theory (Randolph et al. [21]) is adopted.
- Radial stress decreases due to the grout consolidation (Bezuijen, Talmon [22], Talmon [23]).

The investigation load test presented in the chapter 2.4 is re-analyzed using the developed algorithm. Three other load tests in two different localities were further used for verification purposes (Chalmovský [16]). The load – transfer function is shown on Figure 11. The predicted and measured load displacement curves are shown in Figure 12. Slightly higher displacements are predicted, and a reasonable match is reached for the ultimate bearing capacity.

Predicted distributions of skin friction and axial displacements for five different loading stages are shown in Figure 13 and Figure 14. For two last loading stages a shear stress decrease in the front section of the fixed length is already initiated. The tested anchor was equipped by electric resistance gauges placed on the tendon in regular intervals of 1 m. Determination of shear stress profiles was therefore possible. Figure 14 presents the predicted and measured shear stress profile for the last loading stage. Progressive failure propagation is obvious. Predicted peak shear stress is in good match with observation. The fixed length section in the softening regime is longer than predicted.

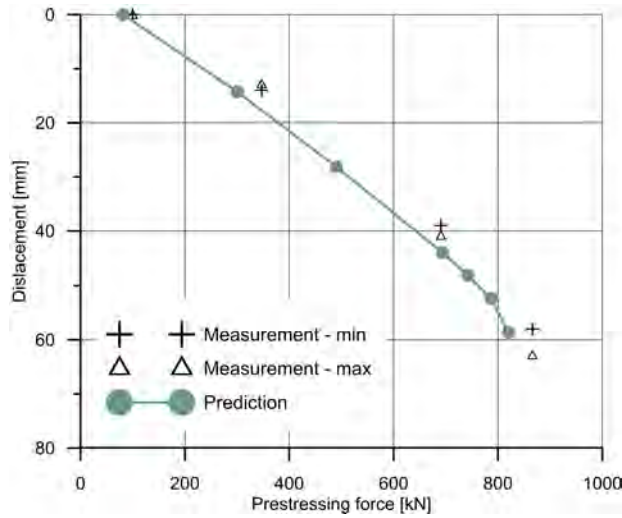


FIGURE 12. Computed and measured load displacement curves.

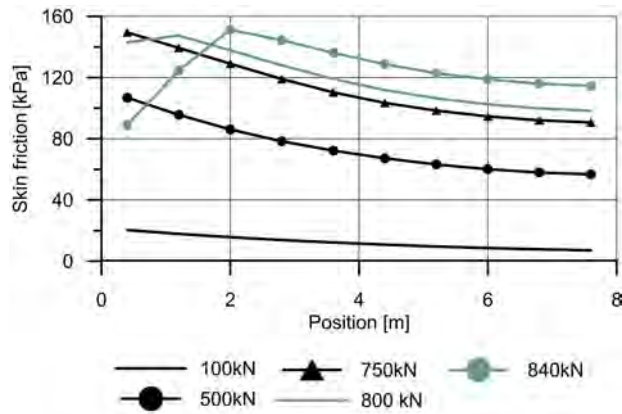


FIGURE 13. Skin friction distributions.

This might be due to slightly higher real bearing capacity (886 kN) which allowed further spreading of the progressive failure.

5. CONCLUSIONS

In order to analyse the non-uniform shear stress distribution along the anchor fixed lengths, three different approaches are presented in the paper: numerical, analytical and experimental. In the first approach the finite element method in combination with the constitutive model involving strain softening was used. The back analysis revealed that ignoring shear stress decrease after peak shear strength is reached may lead to significant bearing capacity overestimation. In-situ loading tests confirmed that the peak and residual bearing capacity should be distinguished. In the presented loading test, the residual peak capacity ratio was 0.55. The newly developed application is based on the load transfer method. Load transfer functions can be assembled employing standard laboratory tests. Detailed information about all three approaches can be found in Chalmovský [16].

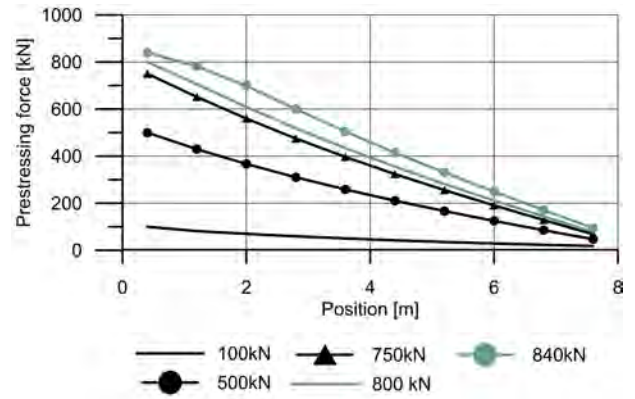


FIGURE 14. Pre-stressing force distributions.

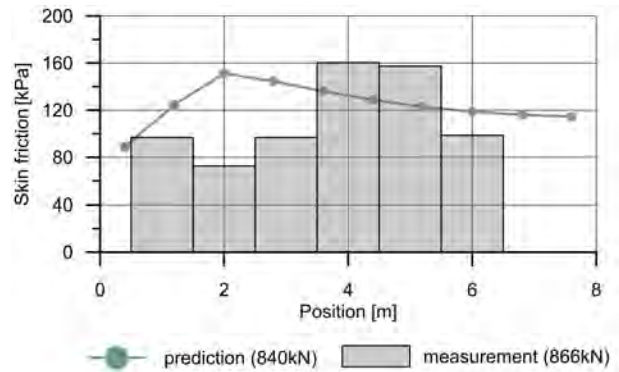


FIGURE 15. Comparison of shear stress distribution for last loading stage.

LIST OF SYMBOLS

- A_{mat} Shear hardening parameter [-]
- c_p Peak cohesion [kPa]
- c_u Undrained cohesion [kPa]
- D Fixed length diameter [m]
- $E_{oed,ref}$ Reference primary oedometer stiffness [kPa]
- $E_{ur,ref}$ Reference unloading-reloading stiffness [kPa]
- f_{eff} Coefficient of effectivity [-]
- h_{soft} Hvorslev surface softening parameter [-]
- K_0 Coefficient of earth pressure at rest [-]
- l_{calc} Internal length for regularization [m]
- L_{fixed} Fixed length [m]
- m Power for stress dependency of stiffness [-]
- OCR Over-consolidation ratio [-]
- p_{ref} Reference stress [kPa]
- T_{ult} Bearing capacity [kN]
- ν_{ur} Poisson ratio for unloading - reloading [-]
- $\sigma_{nc,0}$ Initial pre-consolidation pressure [kPa]
- ϕ_{cs} Critical state friction angle
- ϕ_e Inclination of Hvorslev surface in τ - σ space
- ϕ_p Peak friction angle

ACKNOWLEDGEMENTS

This research was financially supported by the research project of the Ministry of Industry and Trade No. FR-TI4/329.

REFERENCES

- [1] H. Ostermayer. Construction carrying behaviour and creep characteristics of ground anchors. *Proceedings Diaphragm Walls and Anchorages, Inst Civ Eng, London* pp. 141–151, 1975.
- [2] F. Scheele. *Tragfähigkeit von Verpressankern in nichtbindigen Boden Neue Erkenntnisse durch Dehnungsmessungen im Verankerungsbereich*. Technische Universität München, 1981.
- [3] A. D. Barley. The single bore multiple anchor system. *Proc Int Conf: Ground anchorages and anchored structures, London* pp. 65–75, 1997.
- [4] R. I. Woods, K. Barkhordari. The influence of bond stress distribution on ground anchor design. *Proc Int Conf: Ground anchorages and anchored structures, London* pp. 55–64, 1997.
- [5] A. D. Barley. Theory and practice of the single bore multiple anchor system. *Anker in Theorie und Praxis, Proc Int Symposium, Salzburg* pp. 297–301, 1995.
- [6] M. Puller. *Deep excavations: a practical manual*. 2003.
- [7] B. Schadlich. *A Multilaminar Constitutive Model for Stiff Soils, Ph.D. thesis*. Gruppe Geotechnik Graz, Graz University of Technology, Austria, 2012.
- [8] T. Svoboda, D. Mašín. Impact of a constitutive model on inverse analysis of an natm tunnel in stiff clays. *Proc ITA-AITES World Tunnel Congress 2008, Agra, India* 2:627–636, 2008.
- [9] P. W. Mayne, F. H. Kulhawy. K0 ocr relationships in soil. *Proc ASCE J Geotech EngDiv* 108(6):851–872, 1982.
- [10] T. Svoboda, D. Mašín, J. Boháč. Class a predictions of an natm tunnel in stiff clay. *Computers and Geotechnics* 37(6):817–825, 2010.
- [11] R. B. J. Brinkgreve, W. M. Swolfs, E. Engin. Plaxis 2d 2012 - users manual. *Plaxis bv, Delft, The Netherlands* 2012.
- [12] R. B. J. Brinkgreve, W. M. Swolfs, E. Engin. Plaxis 3d 2012 - users manual. *Plaxis bv, Delft, The Netherlands* 2012.
- [13] R. B. J. Brinkgreve. *Geomaterial models and numerical analysis of softening, Ph.D. thesis*. Delft university press, 1994.
- [14] V. Galavi. *A multilaminar model for structured clay incorporating inherent anisotropy and strain softening, Ph.D. thesis*. Gruppe Geotechnik Graz, Graz University of Technology, Austria, 2007.
- [15] P. Mišove. *Construction of pres-tressed ground anchors and their bearing capacity (in Slovak), Ph.D. thesis*. VUIS, Bratislava, 1984.
- [16] J. Chalmovský. *Behaviour analysis of a ground anchor fixed length in fine grained soils (in Czech), Ph.D. thesis*. Brno University of Technology, Department of Geotechnics, 2016.
- [17] H. Coyle, L. C. Reese. Load transfer for axially loaded piles in clay. *Journal of the Soil Mechanics and Foundations Division* 92:1–26, 1966.
- [18] H. Coyle, I. H. Sulaiman. Skin friction for steel piles in sand. *Journal of the Soil Mechanics and Foundations Division* 93(6):261–278, 1967.
- [19] L. M. Kraft, T. Kagawa, R. P. Ray. Theoretical t-z curves. *Journal of the Geotechnical Engineering Division* 107(11):1543–1561, 1981.
- [20] *Building Code Requirements for Structural Concrete (ACI 318) and Commentary*.
- [21] M. F. Randolph, J. S. Steenfelt, C. P. Wroth. The effect of pile type on design parameters for driven piles. *Proc Seventh European Conference on Soil Mechanics and Foundation Engineering 2* pp. 107–114, 1979.
- [22] A. Bezuijen, A. Talmon. Grout pressures around a tunnel lining, influence of grout consolidation and loading on lining. *Proc Underground Space for Sustainable Urban Development (ITA Singapore)* 2004.
- [23] A. Talmon, A. Bezuijen. Simulating the consolidation of tbm grout at noordplaspolder. *Tunnelling and Underground Space Technology* 24(5):493–499, 2009.